BIOCELL
2024 48(11): 1613-1623
ARTICLE

Tech Science Press

Glycyrrhizic acid alleviates lung injury in sepsis through SIRT1/HMGB1 pathway

Bingjie LIN[1]; Xiaobo YING[2]; Chuanling ZHANG[3,*]; Guojun ZHANG[1,*]

[1] Infectious Diseases Department, The First People's Hospital of Fuyang Hangzhou, Hangzhou, 311400, China
[2] Infectious Diseases Department, Affiliated Xiaoshan Hospital, Hangzhou Normal University, Hangzhou, 311201, China
[3] Translational Medicine Laboratory, Affiliated Xiaoshan Hospital, Hangzhou Normal University, Hangzhou, 311201, China

Key words: Glycyrrhizin Acid, Sepsis, sirtuin 1 (SIRT1), high mobility group box 1 (HMGB1)

Abstract: Objectives: This study explores the protective effects of glycyrrhizic acid (GA) on sepsis-induced cellular damage and inflammation in acute lung injury (ALI), specifically through the modulation of the sirtuin 1 (SIRT1) and high mobility group box 1 (HMGB1) pathway. **Methods:** The study employed two experimental models: lipopolysaccharide (LPS)-induced BEAS-2B human lung epithelial cells and cecal ligation and puncture (CLP) rats, to simulate sepsis conditions. The cell model involved treatments with LPS, GA, control siRNA (si-NC), and SIRT1-specific siRNA (si-SIRT1). Evaluations included cell viability, apoptosis, and cytokine production. In the rat model, treatments included GA and the SIRT1 inhibitor EX527, with assessments on lung tissue damage, inflammation, and protein expression using Western blot and co-immunoprecipitation (Co-IP) analysis. **Results:** LPS exposure significantly reduced SIRT1 mRNA levels and cell viability in BEAS-2B cells, which effects were reversed by co-treatment with GA and si-NC but negated by si-SIRT1. LPS also induced apoptosis and increased pro-inflammatory cytokines and HMGB1 expression, which were mitigated by GA and si-NC and exacerbated by si-SIRT1. In CLP rats, GA treatment decreased lung tissue damage, inflammatory cytokines, and HMGB1 expression, and enhanced SIRT1 levels. However, these protective effects were reversed when GA was combined with EX527. **Conclusion:** GA demonstrates significant protective effects against LPS-induced damage and inflammation in lung cells and tissue by modulating the SIRT1-HMGB1 pathway. This suggests that GA could be a potential therapeutic strategy for treating sepsis and related inflammatory conditions.

Introduction

Sepsis is a life-threatening condition triggered by a systemic inflammatory response to infection [1]. It is especially dangerous for critically ill patients, such as those suffering from trauma, burns, shock, or severe infections [1]. One of the most serious complications of sepsis is acute lung injury (ALI), which can result from various causes, including sepsis itself, trauma, and intoxication [2]. ALI is clinically identified by permeability edema, alveolar collapse, and severe, refractory hypoxemia. Among patients older than 15, the incidence rate of ALI is 78.9 per 100,000 people annually, with alarmingly high mortality rates of 38.5% [2]. Like other septic complications, there are currently no specific preventive or therapeutic measures for sepsis-associated ALI. The primary treatment approach is supportive care. Therefore, finding effective treatments for ALI is crucial for improving the survival rates and quality of life of patients with severe sepsis.

High mobility group box 1 (HMGB1) is a protein with dual functions. Extracellularly, it acts as a cytokine, initiating immune responses and participating in inflammatory processes such as sepsis and infection [3]. HMGB1 can activate immune cells like macrophages to produce various cytokines, including interleukin-1β (IL-1β), tumor necrosis factor-α (TNF-α), and interleukin-6 (IL-6) [3]. In a dog sepsis model, serum HMGB1 levels peaked between 8 to 12 h and remained elevated at 24 h [4]. Administering recombinant HMGB1 to mice results in sepsis-like symptoms, and higher doses can be fatal. Conversely, treatment with the HMGB1 synthesis inhibitor

*Address correspondence to: Chuanling Zhang, zhangchuanling@hznu.edu.cn; Guojun Zhang, dayuan1502@163.com
Received: 07 May 2024; Accepted: 09 August 2024;
Published: 07 November 2024

Doi: 10.32604/biocell.2024.053652

sodium butyrate after cecal ligation and puncture (CLP) significantly reduces HMGB1 mRNA expression in multiple tissues and alleviates inflammatory responses, thereby reducing mortality in a sepsis model. This treatment also ameliorated inflammatory responses in liver, kidney, and lung tissues and significantly reduced mouse mortality [5]. Thus, HMGB1, as a late-stage inflammatory mediator, is not only associated with sepsis but also with ALI resulting from sepsis.

Sirtuin 1 (SIRT1) is an NAD^+-dependent histone deacetylase with widespread physiological roles, including the regulation of cellular stress resistance, inflammation, and metabolism [6]. Over the past few years, the potential relationship between SIRT1 and ALI has garnered significant interest [7]. SIRT1 has been shown to exhibit anti-inflammatory properties by inhibiting the transcriptional activities of factors like nuclear factor-kappa B (NF-κB). The integrity of the lung's epithelial and endothelial barriers is crucial for maintaining its function [7]. SIRT1 may play a role in enhancing the tight junction proteins and decreasing permeability, thus maintaining the integrity of these barriers during ALI [8]. Several studies have indicated that the activation of SIRT1 can alleviate the symptoms of ALI, suggesting its potential as a therapeutic target [9]. It was reported that SIRT1, which is an inhibitory transcription factor of HMGB1, blocks the function of HMGB1 by inhibiting the transcription of HMGB1 and thus blocking the function of HMGB1 [9]. However, it's important to note that research in this area is ongoing, and a comprehensive understanding of the exact mechanisms and potential clinical applications remains an active area of study.

Previous studies found that glycyrrhizic acid (GA) could significantly alleviate the lung histopathological state, improve lung function, and reduce the inflammation level of lung tissue in rats with septic ALI [10]. Licorice is a perennial herb of the genus Glycyrrhiza, family Leguminosae. It belongs to the category of tonic herbs, with the functions of tonifying the spleen and benefiting the Qi, easing the emergency and relieving the pain, clearing the heat and detoxifying toxins, regulating all the medicines, and so on. According to the theory of traditional Chinese medicine (TCM), Qi, vital energy, is regarded as a driving force of biological activities in the human body [11]. Qi-invigorating TCMs are widely utilized for the treatment of various disorders, such as obesity, immunosuppression, intestinal flora imbalance, and gastrointestinal diseases, in which Qi is considered to be lessened or depleted [12]. GA, extracted from the root of *Glycyrrhiza glabra*, is the most important active ingredient of *Glycyrrhiza glabra*, which has a variety of biological activities such as anti-inflammatory, hepatoprotective, immunomodulatory, antiviral, and anticancer activities [13]. The mechanism of anti-inflammation has been one of the hotspots of GA research. Studies have shown that GA can exert anti-inflammatory activity through the regulation of multiple inflammation-related signaling pathways. GA can inhibit the activation of the NF-κB signaling pathway, thus reducing the secretion of TNF-α and IL-1β, etc., in macrophages [14]. GA inhibits the lipopolysaccharide (LPS)-activated toll-like receptor 4 (TLR4)/NF-κB signaling pathway, which in turn down-regulates LPS-induced pro-inflammatory gene expression and attenuates inflammatory damage in mouse endometrial epithelial cells [15]. In addition, recent studies have shown that GA activates SIRT1 preventing diabetic nephropathy and improving the pathogenesis of psoriasis [16]. An in-depth investigation of the anti-inflammatory effects of GA in the field of sepsis ALI is of great significance in developing new ideas for the treatment of sepsis ALI.

Given these findings, we hypothesize that GA mitigates septic lung injury by inhibiting HMGB1 expression via the activation of the SIRT1 transcription factor. To test this hypothesis, we will examine the therapeutic effects of GA on septic ALI both *in vitro* and *in vivo*. We will also investigate how GA protects LPS-induced lung cells by modulating HMGB1 through SIRT1 activation. By validating these mechanisms *in vivo*, we aim to elucidate GA's therapeutic potential for septic ALI, providing a theoretical foundation for its clinical application.

Materials and Methods

RNA interference

Human lung epithelial cells, termed BEAS-2B (iCell Bioscience, Inc., iCell-h023, Shanghai, China) were cultured in 6-well plates at 1×10^5/well and subjected to transfection with small interfering RNAs (siRNAs). Using a lipojet transfection kit (SL100468, SignaGen Laboratories, Frederick, MD, USA) following the manufacturer's instructions, siRNAs at a concentration of 40 nm were introduced into the BEAS-2B. The siRNA sequences were designed and synthesized by GenePharma Co., Ltd., (Shanghai, China). Si-NC (Forward: 5′-UUCUCCGAAC GUGUCACGUTT-3′, Reverse: 5′-ACGUGACACGUUC GGAGAATT-3′). si-SIRT1 (Forward: 5′-GUGGCAGA UUGUUAUUAAUTT-3′, Reverse: 5′-AUUAAUAACAA UCUGCCACTT-3′).

Cell culture and grouping

BEAS-2B was maintained in a 37°C incubator with 5% CO_2 using Roswell Park Memorial Institute 1640 medium (RPMI-1640) (11875093, Thermo Fisher Scientific, Inc. Gibco, Waltham, MA, USA) with 10% FBS (A5670701, Thermo Fisher Scientific, Inc.) and 1% penicillin and streptomycin antibiotics (15140122, Thermo Fisher Scientific, Inc.). The results of the PCR assay (data not shown) for mycoplasma demonstrated that BEAS-2B cells were negative for mycoplasma, meaning that the cells were free of mycoplasma infection. The cells in the logarithmic phase were divided into four groups: A: control; B: LPS; C: GA + LPS + si-NC; D: GA + LPS + si-SIRT1. Group A was cultured in a normal RPMI-1640 medium. Group B was added with 10 μg/mL LPS for 12 h [17]; After transfection with si-NC for 24 h, group C was added with 10 μg/mL LPS for 12 h, and cultured in RPMI-1640 medium containing 20 μM GA [18]. After transfection with si-SIRT1 for 24 h, group D was added with 10 μg/mL LPS for 12 h, and cultured in RPMI-1640 medium containing 20 μM GA. After 24 h, cells of each group were collected for use.

Animal adoption

Twenty-four male SD rats, 9 weeks old and with weights ranging from 200–230 g, were procured from Shanghai SLAC Laboratory Animal Co. Ltd., Shanghai, China (License: SCXK (Hu) 2017-0005). These rats were sheltered in Specific Pathogen-Free (SPF) facility at Zhejiang Eyong Pharmaceutical R&D Co., Ltd., Zhejiang, China with conditions maintained at 24°C, 55% humidity, and a 12-h light/dark cycle (License: SYXK (Zhe) 2021-0033). The animal research used is permitted by the Animal Experimentation Ethics Committee of Zhejiang Eyong Pharmaceutical Research and Development Co., Ltd., with license number ZJEY-20220407-02.

Establishment of sepsis model

The CLP method was employed to establish the sepsis model in rats according to the previous study [19]. After inhalation anesthesia, a midline abdominal incision was made. The abdominal hair was shaved, and the skin surface was disinfected with iodophor. A 3 cm incision was made along the midline of the abdomen. The cecum was carefully exteriorized, ensuring no damage to the mesentery or compromise of the integrity of the intestinal wall. A 4.0 suture was used to ligate the cecum 1.5 cm from the cecal tip. Using an 18-gauge needle, the tied section of the cecum was perforated twice, allowing a minimal amount of fecal matter to be squeezed out. The cecum was then repositioned into the abdominal space, and the incision was sutured sequentially. After the operation, we administered physiological saline intraperitoneally to restore fluids. In the Sham group, the entire process was replicated except for the cecal ligation and puncture.

Animal grouping and intervention

After a week of acclimatization, the rats were randomly divided into four groups: A: Sham; B: CLP; C: CLP + GA; D: CLP + GA + EX527 (SIRT1 inhibitor, HY-15452, MCE, New Jersey, USA). Groups B–D were subjected to the CLP procedure as described above. One hour post-surgery, Group C received an intraperitoneal injection of 50 mg/kg GA [20], and Group D received 1 mg/kg EX527 additionally [21]. These injections were administered once daily for 7 days. Physiological saline was delivered intraperitoneally to Group B in an equivalent volume, and sham rats likewise received the same treatment. GA preparation was according to the previous study [22].

Blood and tissue sample collection

A day after the final dosing, rats were anesthetized using isoflurane, and blood samples were collected from the abdominal aorta. The blood was allowed to clot for 1 h and then centrifuged (4°C, 3500 r/min, 10 min) with a machine (Micro17R, Thermo, Waltham, MA, USA) to separate the serum for subsequent analyses. The wet-to-dry weight ratio of the left lung tissue was measured. Lung tissues were harvested, with a portion fixed in 4% formaldehyde (100496, Sigma-Aldrich, St. Louis, MO, USA) for histopathological examination, and another portion was flash-frozen using liquid nitrogen and then stored at −80°C for subsequent experiments.

Lung wet weight/dry weight ratio

From each group, six rats had their left lungs extracted surgically. Any residual blood on these lungs was blotted off, and the wet weight was noted. After drying in an 80°C oven for 48 h, the constant weight (dry weight) was recorded. The severity of pulmonary edema was inferred from the wet weight/dry weight ratio.

Quantitative real-time-polymerase chain reaction (qRT-PCR)

RNA extraction from BEAS-2B cells was accomplished using the TRIzol reagent (15596018CN, Invitrogen, Carlsbad, CA, USA), followed by cDNA synthesis (CW2569, CWBiotech, Beijing, China). QRT-PCR was performed using SYBR Green Master Mix (11201ES08, Yeasen, Shanghai, China) on a StepOnePlus Real-Time PCR System (4376600, Applied Biosystems, Waltham, MA, USA). The $2^{-\Delta\Delta CT}$ approach was used to calculate the relative expression levels of the target genes relative to GAPDH. And the gene of Human SIRT1 sequence is Forward Primer: 5′-TAGCC TTGTCAGATAAGGAAGGA-3′, Reverse Primer: 5′-AC AGCTTCACAGTCAACTTTGT-3′, and Human β-actin (Forward Primer: 5′-GATGACCCAGATCATGTTTGAG, Reverse Primer: 5′-TAATGTCACGCACGATTTCC-3′).

Cell counting kit-8 (CCK8)

Count the BEAS-2B cells in the logarithmic growth phase that were inoculated into a 96-well plate (1×10^4 cells/well), and then set up six replicate wells for each group of treated cells, added 10 μL CCK-8 solution to each well, in addition to drug intervention, and incubated at 37°C for 2 h with CCK8 kit (C0037, Shanghai Beyotime Biotechnology Co., Ltd., Shanghai, China). A 450 nm enzyme labeller (A51119600C, Thermo, Waltham, MA, USA) was used to measure the absorbance value of each well.

Flow cytometry (FCM)

For apoptosis analysis, BEAS-2B cells were tested by the Annexin V-FITC Apoptosis Detection Kit (556549, BD Biosciences, New Jersey, USA). In 6-well plates with a working capacity of 2 mL per well and an inoculation density of 1.2×10^6 cells per well, logarithmic growth stage cells were seeded. Add 100 μL binding buffer, stir well, add 5 μL of Annexin V conjugated with Fluorescein Isothiocyanate (Annexin V-FITC) and 10 μL of Propidium Iodide (PI), respectively, and then add 500 μL of binding buffer. The reaction was then left at room temperature for 15 min without exposure to light. After adding 400 μL of binding buffer, the FCM (643438, BD FACSCalibur, New Jersey, USA) was used for 1 h to measure the apoptosis rate.

Enzyme-linked immunosorbent assay (ELISA)

For the serum of the rats, the blood of rats was collected in a 1.5 mL EP tube with anticoagulant added in advance. The anticoagulant blood was added to a 5 mL EP tube with PBS in advance using an eyedropper. The diluted blood is slowly added into a 15 mL centrifuge tube containing lymphocyte separation solution along the wall of the test tube with an eyedropper. The diluted blood flowing down the wall of the tube is superimposed on the separation solution and forms

an obvious interface with the separation solution. Centrifuge by horizontal centrifuge with a machine (Micro17R, Thermo, Waltham, MA, USA) 2500 rpm, 20 min. Carefully remove the centrifuge tube, use the dropper to absorb the lymphocytes with white flocculent in the middle, and wash them twice with PBS at 1800 rpm for 10 min each time. Discard the supernatant and add 100 μL PBS resuspension cells; Cell samples were taken from each group, and the cell suspension was diluted with PBS, and the cell concentration reached about 1 million/mL. By repeated freezing and thawing, to destroy cells and release cellular components. Centrifuge for 20 min (2000–3000 rpm). Concentrations of cytokines TNF-α, IL-6, and IL-1β in cell supernatants were quantified using ELISA kits (R&D Systems, Minneapolis, MN, USA) listed in Table 1, with absorbance read at 450 nm.

Western blot

Collect tissues and cells. To stop protein deterioration, lyse samples in radio immunoprecipitation assay buffer (Beyotime, P0013B, Shanghai, China) with protease inhibitors (CWBiotech, CW2200S, Beijing, China) and phosphatase inhibitors (Beyotime, ST506, Shanghai, China). The lysates should be centrifuged, and the proteins should be extracted from the supernatant. To ascertain the protein concentration in the samples, use the bicinchoninic acid Protein Assay Kit (Beyotime, PC0020, Shanghai, China). Protein levels should be balanced amongst several samples to achieve comparable loading. Create polyacrylamide gels based on the size of the proteins using 30% acrylamide (Sangon Biotech, B546017-0500, Shanghai, China), 1.5 M Tris pH 8.8 (Biosharp, BL516A, Anhui, China), and 1.0 M Tris pH 6.8 (Biosharp, BL514A, Anhui, China). Proteins are denatured by heating samples with a loading buffer at 95°C. Place a pre-stained protein marker (Solarbio, PR1910, Beijing, China) in each well of the gel along with the same amount of protein. Run the gel at 80 V for as long as samples need to travel through the stacking gel before increasing to 120 V to complete the desired separation. Assemble a transfer sandwich with the gel and a polyvinylidene difluoride (PVDF) membrane (GE Healthcare Life, 10600023, Bloomington, IL, USA). Incubate the membrane in 5% non-fat milk in TBST (Tris-buffered saline with Tween 20). The membrane was treated with primary antibodies (Table 2) overnight at 4°C, followed by HRP-conjugated secondary antibodies (Table 2) at room temperature for 1 h. Membranes were then incubated in 5% non-fat milk in TBST. Using an enhanced chemiluminescence (ECL, P0018S, Beyotime, Shanghai, China) technique, protein bands were seen.

Co-immunoprecipitation (Co-IP)

Cells should be collected and lysed in a solution containing protease/phosphatase inhibitors. To gather the supernatant, centrifuge. Protein A/G Sepharose beads (Santa Cruz Biotechnology, Delaware, USA) should be incubated with lysates for a full hour at 4°C. After centrifugation, collect the lysate that has been cleaned. Lysate and primary antibody are combined, and then incubated at 4°C overnight. Incubate for 3–4 h at 4°C after adding Protein A/G Sepharose beads. Using a centrifuge, remove the supernatant. With cold buffer or PBS, wash the beads. Beads are suspended in 2 × SDS sample buffer and heated for 5 min at 95°C–100°C. SDS-PAGE and Western blotting should be done using the antibodies listed in Table 3.

Hematoxylin and eosin (H&E) staining

Lung tissue sections were deparaffinized, rehydrated, and stained with hematoxylin (H3136, Sigma-Aldrich, St. Louis, MO, USA) for 5 min. After rinsing, sections were counterstained with eosin (E4009, Sigma-Aldrich, St. Louis, MO, USA) for 3 min. Slides were dehydrated, cleared, and mounted. Histological changes were observed under a light microscope (Nikon Eclipse Ci-L, Nikon, Tokyo, Japan). HE scores were performed according to the indexes of alveolar edema, inflammatory cell infiltration, and alveolar wall widening. 0 for no injury, 1 for minor injury, 2 for moderate injury, 3 for severe injury, and 4 for extremely severe injury, and the sum of all scores was the lung tissue pathological score.

Measurement of serum liver and renal index

Serum samples were detected by an automatic biochemical analyzer (3110, Hitachi, Tokyo, Japan) concerning alanine transaminase (ALT), aspartate transaminase (AST), serum creatinine (SCr), blood urea nitrogen (BUN). Myeloperoxidase (MPO) activity in lung tissues was

TABLE 1

ELISA kit information

ELISA kits	Company	Lot
Human IL-6	Ruixin Bio, Quanzhou, China	RX106126H
Human IL-1β		RX106152H
Human TNF-α		RX104793H
Rat IL-6		RX302856R
Rat IL-1β		RX302869R
Rat TNF-α		RX302058R
Myeloperoxidase (MPO)	Jiancheng, Nanjing, China	A044-1-1

TABLE 2

Antibody information

Antibody	Company	Dilution ratio	Lot
SIRT1 antibody	Affinity, OH, USA	1:1000	DF6033
HMGB1 antibody	Affinity, OH, USA	1:1000	AF7020
Anti-rabbit IgG, HRP-linked antibody	CST, Chicago, MA, USA	1:6000	7074
β-actin antibody	Proteintech, Chicago, MA, USA	1:10000	81115-1-RR

TABLE 3

Antibody information

Antibody	Company	Dilution ratio	Lot
Acetylated-Lysine antibody	CST, Chicago, MA, USA	1:1000	9441
HMGB1 antibody	Affinity, OH, USA	1:1000	AF7020
Anti-rabbit IgG, HRP-linked antibody	CST, Chicago, MA, USA	1:6000	7074
β-actin antibody	Proteintech, Chicago, MA, USA	1:10000	81115-1-RR

measured using an MPO test kit. A 2.9 mL solution of o-dianisidine dihydrochloride and hydrogen peroxide was added to 180 L of supernatant after lung tissue had been homogenized and subjected to ultrasonic treatment at 0°C. After 5 min, the reaction was stopped by adding 0.1 mL of hydrochloric acid. Specific photometry was used to determine the absorbance at 400 nm, and the MPO activity was represented as U/g tissue.

TdT-mediated dUTP nick-end labeling (TUNEL) staining

Lung tissue sections were detected using the TUNEL Apoptosis Detection Kit (Roche, 11684795910, Basel, Switzerland). Cells were fixed, permeabilized, and then incubated with the TUNEL reaction mixture. Nuclei were counterstained with DAPI (ab104139, Abcam, Cambridge, UK). Apoptotic cells were visualized and quantified under a fluorescence microscope (Nikon Eclipse Ci-L, Nikon, Japan).

Statistical analysis

For normally distributed data that passed the variance homogeneity test, one-way ANOVA was used to examine the variances among several groups, and Tukey's *post hoc* test was used for direct comparisons. For data that did not follow a normal distribution, the Kruskal-Wallis H test was used. Any differences noted with a p-value < 0.05 were recognized as statistically significant, and all findings were presented as mean standard deviation.

Results

GA exerted a protective effect through SIRT1-HMGB1 in LPS-induced BEAS-2B cells

As depicted in Fig. 1A, there was a significant downregulation of SIRT1 mRNA expression in the LPS than the control group in BEAS-2B cells ($p < 0.01$). Upon treatment with GA and si-NC, the SIRT1 mRNA levels were notably upregulated compared to the LPS group in BEAS-2B cells ($p < 0.01$). However, this upregulation was negated in the presence of GA + LPS + si-SIRT1 in BEAS-2B cells ($p < 0.01$). In Fig. 1B, cell viability of BEAS-2B cells was assessed using the CCK8 assay. LPS treatment resulted in a marked decrease in cell viability than the control group. Remarkably, co-treatment with GA in LPS-stimulated cells significantly enhanced cell viability compared to the LPS group ($p < 0.01$). This protective effect was abrogated upon the introduction of si-SIRT1 compared to the GA + LPS + si-NC ($p < 0.01$). FCM analysis, as shown in Fig. 1C,D, revealed that LPS treatment induced a higher rate of apoptosis compared to the control group. Interestingly, the GA + LPS + si-NC group exhibited a significant reduction in apoptotic cells compared to the LPS group. The introduction of si-SIRT1 reversed this protective effect ($p < 0.01$). ELISA results, as presented in Fig. 1E, demonstrated that pro-inflammatory cytokines, including TNF-α, IL-6, and IL-1β, were significantly elevated in the LPS group compared to the control in BEAS-2B cells ($p < 0.01$). The GA + LPS + si-NC group exhibited a significant reduction in these cytokines than the LPS group in BEAS-2B cells. In contrast, the introduction of si-SIRT1 negated this anti-inflammatory effect in BEAS-2B cells ($p < 0.01$).

In Fig. 2A,B, Western blot analysis confirmed that the relative expression of SIRT1 was significantly diminished in the LPS group than control in BEAS-2B cells ($p < 0.01$). The GA + LPS + si-NC treatment resulted in a significant upregulation of SIRT1 expression compared to the LPS group in BEAS-2B cells ($p < 0.01$). Conversely, the introduction of si-SIRT1 counteracted the effect observed in the GA + LPS + si-NC group in BEAS-2B cells ($p < 0.01$). Moreover, the expression pattern of HMGB1 was inversely proportional to that of SIRT1 proteins in BEAS-2B cells ($p < 0.01$, respectively). In our study, we used Co-IP to assess the acetylation levels of HMGB1 because acetylation is a key post-translational modification that affects the function and

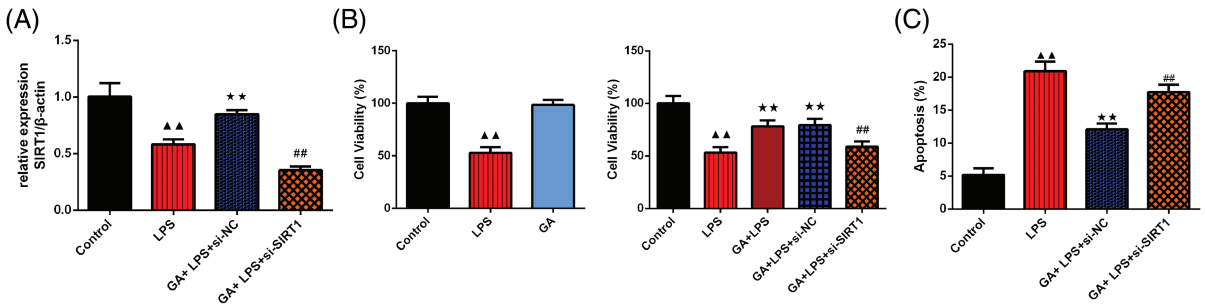

FIGURE 1. (Continued)

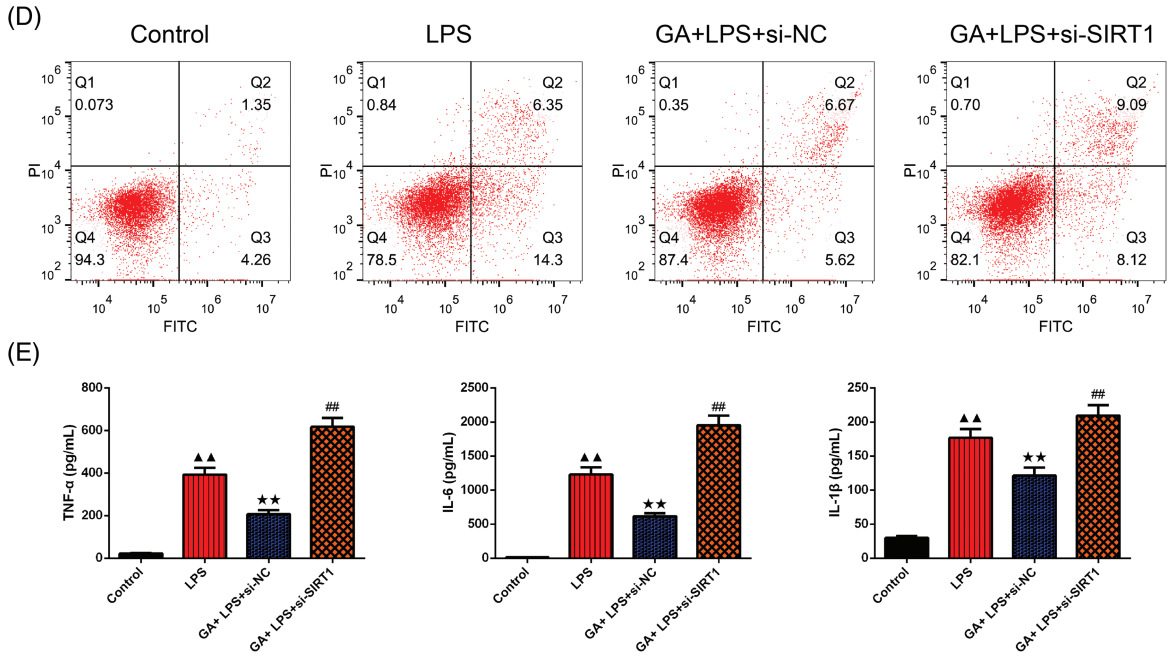

FIGURE 1. GA exerted a protective effect through SIRT1 in LPS-induced BEAS-2B cells. (A) qRT-PCR was used to test the relative *SIRT1* mRNA expression in each group of BEAS-2B cells, $n = 3$ in each group; (B) CCK8 was used to evaluate the cell viability of the in each group of BEAS-2B cells, $n = 6$ in each group; (C and D) FCM was used to testify the apoptosis rate in each group of BEAS-2B cells, and the graph was shown, $n = 3$ in each group; (E) ELISA kits were used to testify the expression of TNF-α, IL-6, IL-1β in each group of BEAS-2B cells, $n = 6$ in each group, $^{▲▲}p < 0.01$ *vs.* control group, $^{**}p < 0.01$ *vs.* LPS group, $^{\#\#}p < 0.01$ *vs.* GA + LPS + si-NC group.

Note: Glycyrrhizic acid: GA; SIRT1: Sirtuin 1; LPS: lipopolysaccharide; qRT-PCR: quantitative real time polymerase chain reaction; CCK8: Cell Counting Kit-8; FCM: Flow CytoMetry; ELISA: enzyme-linked immunosorbent assay; TNF-α: Tumor Necrosis Factor-α; IL-6: interleukin-6; IL-1β: interleukin-1β.

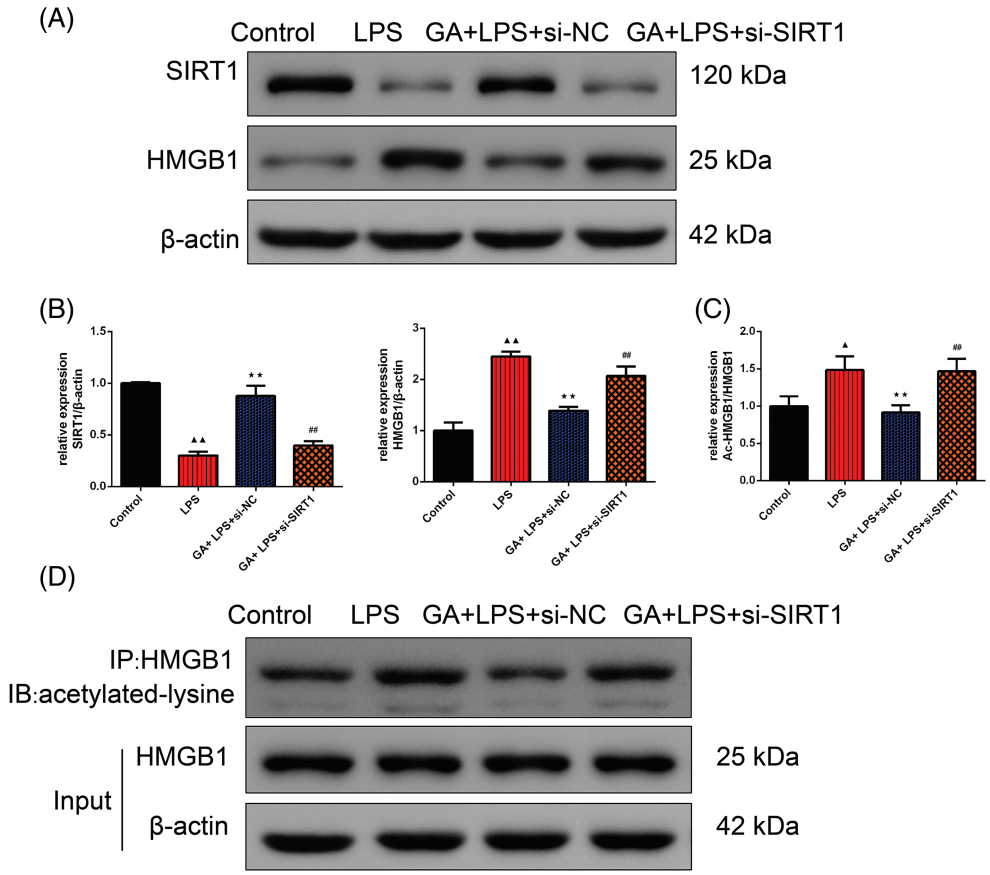

FIGURE 2. GA exerted a protective effect through SIRT1-HMGB1 in LPS-induced BEAS-2B cells. (A and B) Western blot was applied to test the relative expression of the SIRT1 and HMGB1 in each group of BEAS-2B cells, $n = 3$ in each group; (C and D) Co-IP was used to evaluate the inner relation of the SIRT1 and HMGB1 in each group of BEAS-2B cells, $n = 3$ in each group; $^{▲}p < 0.05$ and $^{▲▲}p < 0.01$ *vs.* control group, $^{**}p < 0.01$ *vs.* LPS group, $^{\#\#}p < 0.01$ *vs.* GA + LPS + si-NC group.

Note: Glycyrrhizic acid: GA; SIRT1: Sirtuin 1; LPS: lipopolysaccharide; HMBG1: high mobility group box 1; Co-IP: Co-Immunoprecipitation.

localization of HMGB1. Elevated acetylation of HMGB1 is associated with its release from the nucleus to the cytoplasm and extracellular space, where it can act as a pro-inflammatory mediator, exacerbating inflammation. As depicted in Fig. 2C,D, Co-IP analysis confirmed that in relative to the control group, the expression level of acetylated HMGB1 protein in BEAS-2B cells of the LPS group was significantly elevated ($p < 0.05$). In comparison to the LPS group, the GA+ LPS + si-NC group exhibited a significant reduction in the expression level of acetylated HMGB1 protein in BEAS-2B cells ($p < 0.01$). Relative to the GA + LPS + si-NC group, the GA + LPS + si-SIRT1 group showed a significant increase in the expression level of acetylated HMGB1 protein in BEAS-2B cells ($p < 0.01$).

GA exerted a protective effect through SIRT1-HMGB1 in CLP rats

As depicted in Fig. 3A, there was a significant upregulation of the wet/dry weight ratio in the CLP group than sham group ($p < 0.01$). Upon treatment with GA, the wet/dry weight ratio was notably downregulated compared to the CLP rats ($p < 0.01$). However, this downregulation was negated in the presence of CLP + GA + EX527 ($p < 0.01$). As can be seen from Fig. 3B,C, the lung tissue morphology and structure of sham rats were basically normal, with no model damage. In CLP rats, lung tissue injury was severe, inflammatory cells were infiltrated, alveolar walls were widened, and edema and congestion occurred. Compared with CLP rats, the CLP + GA group reduced lung tissue injury, inflammatory cell infiltration, alveolar wall widening, edema, and congestion. Compared with CLP + GA rats, the lung tissue injury of CLP + GA + EX527 rats was deepened. Similarly, compared with the sham group, HE scores, the expression of the ALT, AST, SCr, BUN, MPO, IL-6, IL-1β, and TNF-α tested by the automatic biochemical analyzer and ELISA kits, and TUNEL-positive cell rate in lung tissue of CLP rats was significantly increased (Fig. 3D–G, Fig. 4A,B, $p < 0.01$).

Compared with CLP rats, HE scores, the expression of the ALT, AST, SCr, BUN, MPO, IL-6, IL-1β and TNF-α, and TUNEL-positive cell rate in lung tissue of the CLP + GA group was significantly decreased ($p < 0.01$). Compared with CLP + GA rats, HE score, the expression of the ALT, AST, SCr, BUN, MPO, IL-6, IL-1β and TNF-α, and TUNEL-positive cell rate in lung tissue of CLP + GA + EX527 rat was significantly increased ($p < 0.05$ or $p < 0.01$). In Fig. 4C,D, Western blot analysis confirmed that the relative expression of SIRT1 was significantly diminished in the CLP rats than in sham rats ($p < 0.01$). The CLP + GA treatment resulted in a significant upregulation of SIRT1 expression than sham rats ($p < 0.01$). Conversely, the introduction of EX527 counteracted the effect observed in the CLP + GA rats ($p < 0.01$). Moreover, the expression pattern of HMGB1 was inversely proportional to that of SIRT1 proteins ($p < 0.01$).

Discussion

The intricate relationship between cellular damage, inflammation, and the underlying molecular pathways in sepsis has been a focal point of numerous studies. Our findings shed light on the pivotal role of the SIRT1-HMGB1 pathway in mediating the effects of GA in LPS-induced BEAS-2B cells and CLP rats, offering a potential therapeutic target for sepsis and related conditions.

Sepsis disease established by the CLP model was certified by the pathology change stained by the HE and the higher wet/dry weight radio of the lung tissue and the injuries of other organs (liver and kidney) with the higher expression of the ALT, AST, SCr, and BUN in peripheral blood of rats and higher expression of the inflammatory factors IL-6, IL-1β, and TNF-α. Li et al. [23] supported that CLP induced the injury of the liver with higher expression of the ALT, AST, and the protective treatment successfully downregulated the expression of the ALT, AST, and IL-6, IL-1β, and TNF-α. Furthermore, the study claimed that GA protects experimental sepsis rats against ALI and inflammation [20].

The significant downregulation of SIRT1 mRNA expression in the LPS group underscored the detrimental effects of LPS on cellular health in BEAS-2B cells. SIRT1 has been previously implicated in various cellular processes, including inflammation, apoptosis, and metabolism in lung injury [24]. Targeting SIRT1 may provide a unique treatment option to reduce ALI during heat stroke, according to Chen's report that the SIRT1/p53 axis mediated ferroptosis in heat stroke-ALI [25]. Additionally, SIRT1 can greatly reduce LPS-induced macrophage apoptosis and sepsis-related lung damage. Its suppression of the endoplasmic reticulum (ER) stress response is directly responsible for this protective effect [26]. It was found that GA and si-NC co-treatment effectively upregulated SIRT1 mRNA levels, enhancing cell viability, which aligns with previous studies suggesting the protective role of SIRT1 against cellular stress [27].

The inverse relationship between SIRT1 and HMGB1 expressions, as revealed by our Western blot and Co-IP analyses, is particularly intriguing. Similarly, it was reported that baicalin inhibited HMGB1 release via the SIRT1/HMGB1 pathway thereby ameliorating cognitive deficits, and suppressing LPS-induced neuroinflammatory responses, suggesting the relation of the SIRT1 and HMGB1 in neuroinflammation [28]. HMGB1, a nuclear protein, has been identified as a late mediator of lethal systemic inflammation in sepsis [29]. Its elevated expression in the LPS group and subsequent reduction with GA treatment suggest that GA might exert its protective effects by modulating the SIRT1-HMGB1 axis. This is further supported by the exacerbated effects observed upon the introduction of si-SIRT1, which negated the protective effects of GA. Consistently, evidence suggests reduced neuroinflammation and improved neurocognitive deficits in LPS-induced mice via SIRT1-mediated HMGB1 downregulation. Elevated HMGB1 levels in serum but decreased intracellular levels in the later stages of septic mice have been observed [30]. The acetylation of HMGB1 is crucial for its movement from the nucleus to the cytoplasm and its subsequent external secretion in kidney cells, exacerbating sepsis-related acute kidney injuries.

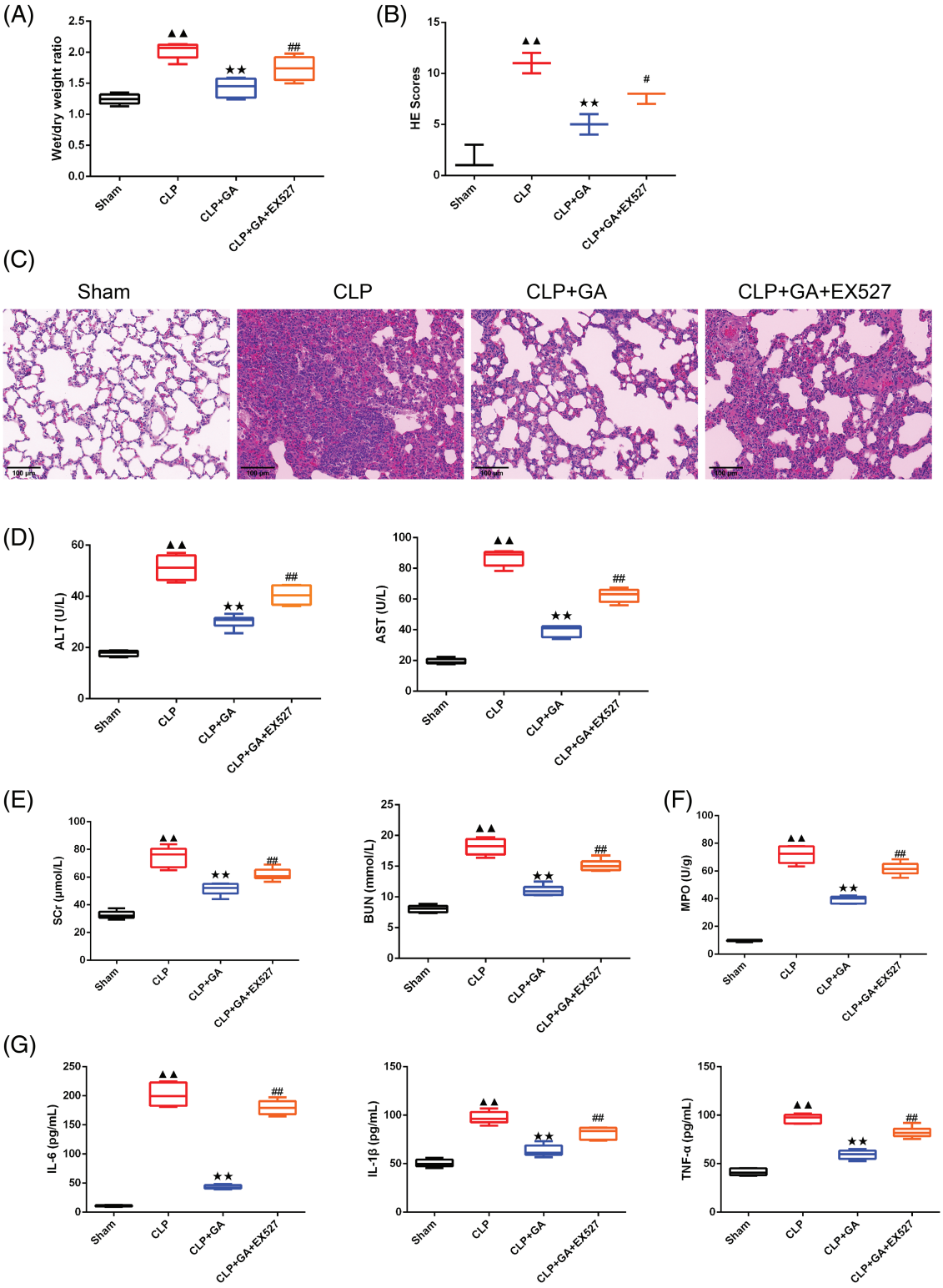

FIGURE 3. GA exerted a protective effect through SIRT1 in CLP rats. (A) Wet-dry ratio was used to detect the wet/dry weight ratio of lung tissue in rats, $n = 6$ in each group; (B and C) The representative image of the pathology in the lung tissue and HE score in rats were recorded, $n = 3$ in each group; (D–F) The contents of ALT, AST, SCr and BUN in peripheral blood of rats in each group were detected by automatic biochemical analyzer; and the kit was used to detect MPO activity of lung tissue in rats, $n = 6$ in each group; (G) The levels of IL-6, IL-1β and TNF-α in peripheral blood in rats were detected by ELISA, $n = 6$ in each group. $^{▲▲}p < 0.01$ *vs.* sham group, $^{**}p < 0.01$ *vs.* CLP group, $^{\#\#}p < 0.01$ *vs.* CLP + GA group.

Note: Glycyrrhizic acid: GA; SIRT1: Sirtuin 1; CLP: Cecum Ligation and Puncture; HE: hematoxylin and eosin; ALT: alanine transaminase; AST: aspartate transaminase; SCr: serum creatinine; BUN: blood urea nitrogen; MPO: myeloperoxidase; ELISA: enzyme-linked immunosorbent assay; TNF-α: Tumor Necrosis Factor-α; IL-6: interleukin-6; IL-1β: interleukin-1β.

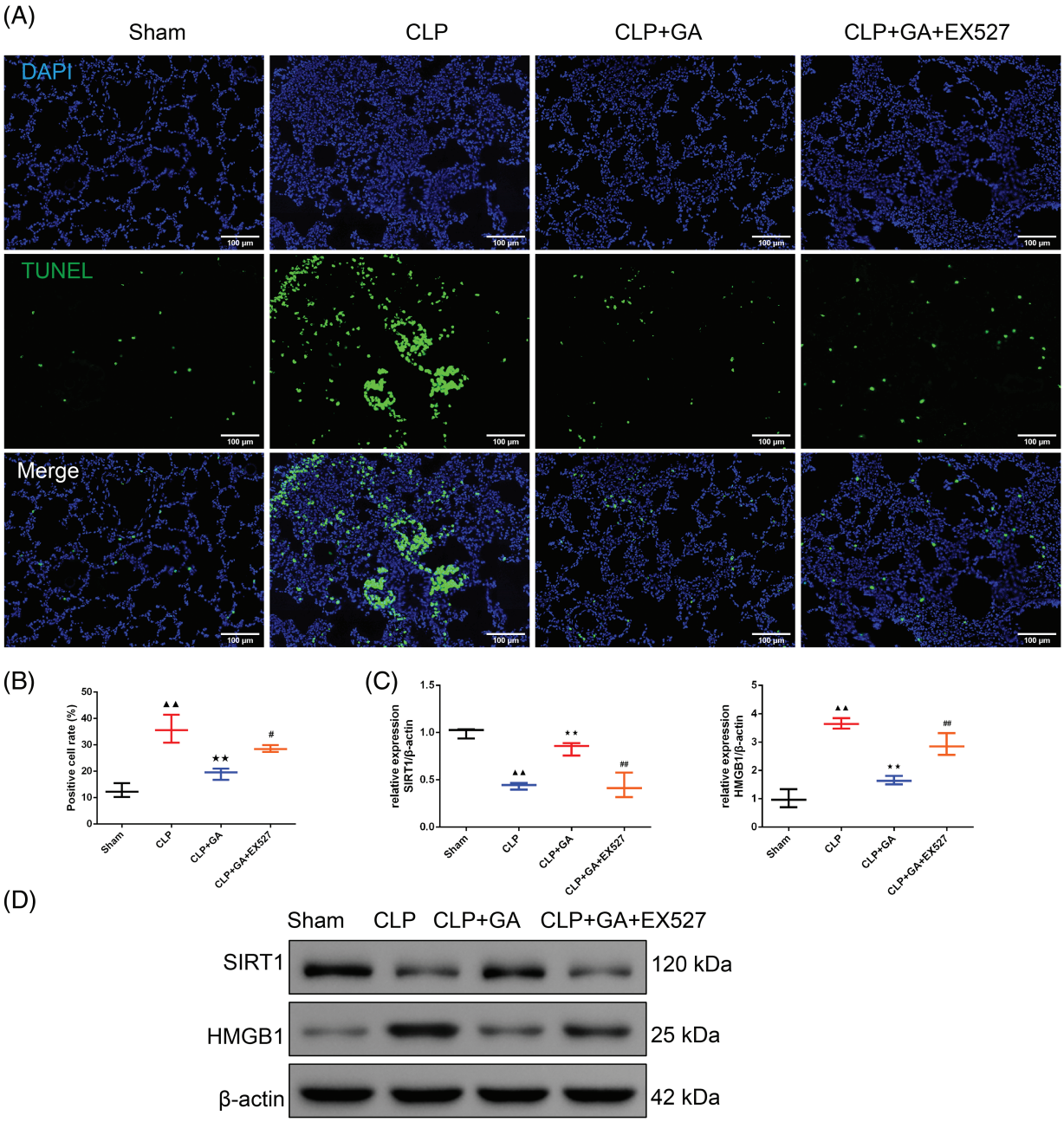

FIGURE 4. GA exerted a protective effect through SIRT1-HMGB1 in CLP rats. (A and B) TUNEL staining was used to evaluate the percentage of the apoptosis cell in lung tissue in rats (magnification 200 ×, scale bar: 100 μm), $n = 3$ in each group; (C and D) Western blot was applied to test the relative expression of the SIRT1 and HMGB1 in rats, $n = 3$ in each group; $^{▲▲}p < 0.01$ *vs.* sham group, $^{**}p < 0.01$ *vs.* CLP group, $^{\#}p < 0.05$ and $^{\#\#}p < 0.01$ *vs.* CLP + GA group.

Note: Glycyrrhizic acid: GA; SIRT1: Sirtuin 1; CLP: Cecum Ligation and Puncture; HMBG1: high mobility group box 1.

Interestingly, SIRT1 interacts with HMGB1, particularly at the deacetylated lysine sites K28, K29, and K30, diminishing inflammatory signaling [9].

In the *in vivo* model, the CLP rats mirrored the cellular findings, with GA treatment significantly reducing lung tissue damage and inflammation. The lung, being a primary organ affected in sepsis, showcases the potential systemic benefits of GA treatment. The reversal of these benefits upon EX527 administration, a known SIRT1 inhibitor [31], further strengthens the argument for the SIRT-HMGB1 pathway's centrality in mediating GA's effects. The study by Honda et al. [32] investigates the anti-inflammatory effects of saponin GL and chalcone ILG from *Glycyrrhiza uralensis*, focusing on their ability to inhibit toll-like receptor 4 (TLR4)/myeloid differentiation protein-2 (MD-2) complex signaling, thereby suppressing NF-κB and mitogen-activated protein kinase (MAPK) pathways and reducing cytokine production. Therefore, our study explores the protective effects of GA on sepsis-induced ALI by modulating the SIRT1-HMGB1 pathway. Using LPS-induced human lung epithelial cells and CLP rat models, we demonstrate that GA reduces lung tissue damage, inflammation, and apoptosis by enhancing SIRT1 levels and decreasing HMGB1 expression. While both studies highlight the therapeutic potential of compounds from *Glycyrrhiza uralensis*, they focus on different molecular mechanisms and experimental models.

In addition, the psoriasis study focuses on glycyrrhizin's ability to improve psoriasis symptoms by inhibiting IL-17A and interferon-gamma (IFN-γ) expression and suppressing signal transducer and activator of transcription 3 (STAT3) pathway activation through upregulating SIRT1 [27]. Moreover, using EX-527 on IL-17A-HaCaT cells and silencing SIRT1 expression echoed these outcomes [27]. In fact, our research investigates GA in sepsis-induced ALI, showing that GA enhances SIRT1 levels and reduces inflammation and lung damage via the SIRT1-HMGB1 pathway. While both studies highlight anti-inflammatory effects, they target different conditions and mechanisms. GA enhances SIRT1 activity, which leads to the deacetylation and inactivation of HMGB1, reducing its release and pro-inflammatory effects. This inhibition of HMGB1 release prevents the activation of inflammatory pathways and the recruitment of immune cells to the lungs. Additionally, GA downregulates pro-inflammatory cytokines and boosts antioxidant defenses, thereby reducing inflammation and oxidative stress in lung tissue. However, while our findings are promising, they also raise further questions. The exact mechanism through which GA modulates the SIRT1-HMGB1 pathway remains to be elucidated. Additionally, the potential side effects and optimal dosages of GA in clinical settings warrant further investigation.

In conclusion, our study underscored the potential of GA as a therapeutic agent against sepsis-induced cellular damage and inflammation, acting through the SIRT-HMGB1 pathway. Future studies delving deeper into this pathway and the broader implications of GA treatment could pave the way for innovative therapeutic strategies against sepsis.

Acknowledgement: None.

Funding Statement: This work was supported by the (Zhejiang Province Traditional Chinese Medicine Science and Technology Plan Project under Grant (No. 2023ZL140).

Author Contributions: Conception and design of the research: Guojun Zhang, Chuanling Zhang; Acquisition of data: Xiaobo Ying; Analysis and interpretation of data: Bingjie Lin; Statistical analysis: Bingjie Lin, Xiaobo Ying; Obtaining funding: Bingjie Lin; Drafting the manuscript: Bingjie Lin; Revision of manuscript for important intellectual content: Guojun Zhang, Chuanling Zhang. All authors reviewed the results and approved the final version of the manuscript.

Availability of Data and Materials: The datasets generated during and/or analyzed during the current study are available from the corresponding author on reasonable request.

Ethics Approval: The animal research used permitted by the Animal Experimentation Ethics Committee of Zhejiang Eyong Pharmaceutical Research and Development Co., Ltd., with license number ZJEY-20220407-02 and consent to participate and publish.

Conflicts of Interest: The authors declare that they have no conflicts of interest to report regarding the present study.

References

1. Purcarea A, Sovaila S. Sepsis, a 2020 review for the internist. Rom J Intern Med. 2020;58(3):129–37. doi:10.2478/rjim-2020-0012.
2. He YQ, Zhou CC, Yu LY, Wang L, Deng JL, Tao YL, et al. Natural product derived phytochemicals in managing acute lung injury by multiple mechanisms. Pharmacol Res. 2021;163:105224. doi:10.1016/j.phrs.2020.105224.
3. Chen R, Kang R, Tang D. The mechanism of HMGB1 secretion and release. Exp Mol Med. 2022;54(2):91–102. doi:10.1038/s12276-022-00736-w.
4. Sun J, Shi S, Wang Q, Yu K, Wang R. Continuous hemodiafiltration therapy reduces damage of multi-organs by ameliorating of HMGB1/TLR4/NFκB in a dog sepsis model. Int J Clin Exp Pathol. 2015;8(2):1555–64.
5. Kwon WY, Suh GJ, Kim KS, Jo YH, Lee JH, Kim K, et al. Glutamine attenuates acute lung injury by inhibition of high mobility group box protein-1 expression during sepsis. Br J Nutr. 2010;103(6):890–8. doi:10.1017/S0007114509992509.
6. Dai H, Sinclair DA, Ellis JL, Steegborn C. Sirtuin activators and inhibitors: promises, achievements, and challenges. Pharmacol Ther. 2018;188:140–54. doi:10.1016/j.pharmthera.2018.03.004.
7. Zhang Y, Zhang H, Li S, Huang K, Jiang L, Wang Y. Metformin alleviates LPS-induced acute lung injury by regulating the SIRT1/NF-κB/NLRP3 pathway and inhibiting endothelial cell pyroptosis. Front Pharmacol. 2022;13:801337. doi:10.3389/fphar.2022.801337.
8. Li X, Jamal M, Guo P, Jin Z, Zheng F, Song X, et al. Irisin alleviates pulmonary epithelial barrier dysfunction in sepsis-induced acute lung injury via activation of AMPK/SIRT1 pathways. Biomed Pharmacother. 2019;118:109363. doi:10.1016/j.biopha.2019.109363.
9. Wei S, Gao Y, Dai X, Fu W, Cai S, Fang H, et al. SIRT1-mediated HMGB1 deacetylation suppresses sepsis-associated acute kidney injury. Am J Physiol Renal Physiol. 2019;316(1):F20–31. doi:10.1152/ajprenal.00119.2018.
10. Zhu L, Wei M, Yang N, Li X. Glycyrrhizic acid alleviates the meconium-induced acute lung injury in neonatal rats by inhibiting oxidative stress through mediating the Keap1/Nrf2/HO-1 signal pathway. Bioengineered. 2021;12(1):2616–26. doi:10.1080/21655979.2021.1937445.
11. Liu HX, Lian L, Hou LL, Liu CX, Ren JH, Qiao YB, et al. Herb pair of Huangqi-Danggui exerts anti-tumor immunity to breast cancer by upregulating PIK3R1. Animal Model Exp Med. 2024;7(3):234–58. doi:10.1002/ame2.v7.3.
12. Wang XM, Li XB, Peng Y. Impact of Qi-invigorating traditional Chinese medicines on intestinal flora: a basis for rational choice of prebiotics. Chin J Nat Med. 2017;15(4):241–54.
13. Selyutina OY, Polyakov NE. Glycyrrhizic acid as a multifunctional drug carrier—from physicochemical properties to biomedical applications: a modern insight on the ancient drug. Int J Pharm. 2019;559:271–9. doi:10.1016/j.ijpharm.2019.01.047.
14. Mao Y, Wang B, Xu X, Du W, Li W, Wang Y. Glycyrrhizic acid promotes M1 macrophage polarization in murine bone marrow-derived macrophages associated with the activation of JNK and NF-κB. Mediat Inflamm. 2015;2015:372931. doi:10.1155/mi.v2015.1.
15. Wang XR, Hao HG, Chu L. Glycyrrhizin inhibits LPS-induced inflammatory mediator production in endometrial epithelial cells. Microb Pathog. 2017;109:110–3. doi:10.1016/j.micpath.2017.05.032.

16. Hou S, Zhang T, Li Y, Guo F, Jin X. Glycyrrhizic acid prevents diabetic nephropathy by activating AMPK/SIRT1/PGC-1α signaling in db/db mice. J Diabetes Res. 2017;2017:2865912. doi:10.1155/2017/2865912.
17. Zhou M, Meng L, He Q, Ren C, Li C. Valsartan attenuates LPS-induced ALI by modulating NF-κB and MAPK pathways. Front Pharmacol. 2024;15:1321095. doi:10.3389/fphar.2024.1321095.
18. Zuo Z, He L, Duan X, Peng Z, Han J. Glycyrrhizic acid exhibits strong anticancer activity in colorectal cancer cells via SIRT3 inhibition. Bioengineered. 2022;13(2):2720–31. doi:10.1080/21655979.2021.2001925.
19. Ghafil FA, Majeed SA, Qassam H, Mardan HW, Hadi NR. Nephroprotective effect of gamma-secretase inhibitor on sepsis-induced renal injury in mouse model of CLP. Wiad Lek. 2023;76(1):122–30. doi:10.36740/WiadLek.
20. Shen J, Hua Z, Chai Y. Glycyrrhizic acid protects experimental sepsis rats against acute lung injury and inflammation. Evid Based Complement Alternat Med. 2022;2022:3571800. doi:10.1155/2022/3571800.
21. Albasher G, Alkahtani S, Al-Harbi LN. Urolithin a prevents streptozotocin-induced diabetic cardiomyopathy in rats by activating SIRT1. Saudi J Biol Sci. 2022;29(2):1210–20. doi:10.1016/j.sjbs.2021.09.045.
22. Tsai JJ, Pan PJ, Hsu FT, Chung JG, Chiang IT. Glycyrrhizic acid modulates apoptosis through extrinsic/intrinsic pathways and inhibits protein Kinase B- and extracellular signal-regulated Kinase-mediated metastatic potential in hepatocellular carcinoma *in vitro* and *in vivo*. Am J Chin Med. 2020;48(1):223–44. doi:10.1142/S0192415X20500123.
23. Li Z, Liu T, Feng Y, Tong Y, Jia Y, Wang C, et al. PPARγ alleviates sepsis-induced liver injury by inhibiting hepatocyte pyroptosis via inhibition of the ROS/TXNIP/NLRP3 signaling pathway. Oxid Med Cell Longev. 2022;2022:1269747. doi:10.1155/2022/1269747.
24. Wang W, Wang Z, Yang X, Song W, Chen P, Gao Z, et al. Rhein ameliorates septic lung injury and intervenes in macrophage metabolic reprogramming in the inflammatory state by Sirtuin 1. Life Sci. 2022;310:121115. doi:10.1016/j.lfs.2022.121115.
25. Chen H, Lin X, Yi X, Liu X, Yu R, Fan W, et al. SIRT1-mediated p53 deacetylation inhibits ferroptosis and alleviates heat stress-induced lung epithelial cells injury. Int J Hyperthermia. 2022;39(1):977–86. doi:10.1080/02656736.2022.2094476.
26. Wang F, Ma J, Wang J, Chen M, Xia H, Yao S, et al. SIRT1 ameliorated septic associated-lung injury and macrophages apoptosis via inhibiting endoplasmic reticulum stress. Cell Signal. 2022;97:110398. doi:10.1016/j.cellsig.2022.110398.
27. Qiong H, Han L, Zhang N, Chen H, Yan K, Zhang Z, et al. Glycyrrhizin improves the pathogenesis of psoriasis partially through IL-17A and the SIRT1-STAT3 axis. BMC Immunol. 2021;22(1):34. doi:10.1186/s12865-021-00421-z.
28. Li Y, Liu T, Li Y, Han D, Hong J, Yang N, et al. Baicalin ameliorates cognitive impairment and protects microglia from LPS-induced neuroinflammation via the SIRT1/HMGB1 pathway. Oxid Med Cell Longev. 2020;2020:4751349. doi:10.1155/2020/4751349.
29. Xue J, Suarez JS, Minaai M, Li S, Gaudino G, Pass HI, et al. HMGB1 as a therapeutic target in disease. J Cell Physiol. 2021;236(5):3406–19. doi:10.1002/jcp.30125.
30. Lee IC, Kim DY, Bae JS. Sulforaphane reduces HMGB1-mediated septic responses and improves survival rate in septic mice. Am J Chin Med. 2017;45(6):1253–71. doi:10.1142/S0192415X17500690.
31. Wang T, Li X, Sun SL. EX527, a Sirt-1 inhibitor, induces apoptosis in glioma via activating the p53 signaling pathway. Anticancer Drugs. 2020;31(1):19–26. doi:10.1097/CAD.0000000000000824.
32. Honda H, Nagai Y, Matsunaga T, Saitoh S, Akashi-Takamura S, Hayashi H, et al. Glycyrrhizin and isoliquiritigenin suppress the LPS sensor toll-like receptor 4/MD-2 complex signaling in a different manner. J Leukoc Biol. 2012;91(6):967–76. doi:10.1189/jlb.0112038.